



Prediction of Stress, Strain, and Deformation in AC Frame of Shunting Locomotive with Exceptional Load

Anung Dwi Prasetyo^{1*}, Dadang Sanjaya Atmaja², Ilham Satrio Utomo³,
Willy Artha Wirawan⁴

Author Affiliation

^{1,2,3,4}Indonesian Railway Polytechnic, Tirta Raya Street, Manguharjo, 63161 Madiun, Indonesia

Author Email

dwi.tmp20203102@ppi.ac.id

Abstract. This study used the method of finite element for modeling and analyzing the structure of the AC frame. Moreover, software was also applied to do a calculation and displayed an illustration of a prediction of the real phenomenon. The process of modeling the AC frame was carried out by utilizing software inventor, and followed by a meshing process and a simulation by employing software ansys. The simulation was done by giving four different load cases based on the standard of UIC 566 that regulates the calculation of load for each component of the train car body. This study has three outputs comprised of von-mises stress, maximum vertical deflection, and value of safety factor. Based on the simulation, the combined load potentially could cause a maximum stress at the stiffener frame AC namely 81,2, MPa, and maximum vertical deflection was 1,015 mm at the carline due to longitudinal load. In addition, the value of the minimum safety factor occurred when the combined load reached 3.0176 during the simulation of the AC frame. The value is considered safe due to under the permitted voltage based on the regulation of the Ministry of Transportation Number 175 in the year of 2015 namely 75% of 245 MPa (allowed voltage for material SS400), namely 183,75 MPa.

Keywords: Finite Element Method, Stress-Strain, Deformation, Exceptional load.

1 Introduction

To meet the needs and progress in the field of transportation, technological developments and innovation are needed, as well as in rail transportation. In line with existing developments, of course, production in the manufacture of railway facilities must also increase both in terms of quality and quantity. PT Industri Kereta Api (Persero) also known as PT A is a manufacturer of railway facilities that produces various of railroad products. One of PT INKA's products is the Shunting Locomotive. The Shunting Locomotive is a self-propelled rail system and is used to tow and/or push trains, carriages, or special, equipment.

The PPI Locomotive Shunting consists of the main construction in the form of a car body and a bogie. A body is used as a space used by passengers and goods and can protect what is inside from collisions, weather changes, or outside noise. The car body

© The Author(s) 2024

A. Pradipta et al. (eds.), *Proceedings of the 2nd International Conference on Railway and Transportation 2023 (ICORT 2023)*, Advances in Engineering Research 231,

https://doi.org/10.2991/978-94-6463-384-9_24

from Shunting Locomotive PPI consists of a roof, side walls, and an underframe consisting of a middle frame and bolsters. The roof of the train (train roof) is a welded steel construction with a longitudinal and horizontal arrangement. The train roof consists of transverse (carline) and longitudinal (purline) steel frames and roof panels.

The AC frame on the roof frame needs to be analyzed separately to measure how strong the AC frame is in supporting the existing load without deformation and can withstand the exceptional load on the geometry and material used [1]. The AC frame acts as a foundation that will support the frame and parts of the AC components. Therefore, the AC frame of the train is required to meet the specified standards so that it can support the loads and forces that occur on the frame. The test standard used for AC frames refers to the Union Internationale Des Chemins De Fer 566 (UIC 566) Standard for loading on Carbody components [2]. The main objective of this study was to determine the stress and amount of displacement by examining the Air Conditioning Frame strength under the required loading and operating conditions. The AC frame design was based on the Shunting Locomotive PPI reference that was produced by PT Industri Kereta Api (INKA).

2 Research Method

The research method used is quasi-experimental by conducting design simulations using FEM (finite element method) software. The output values generated from this simulation will be validated based on the UIC 566 standard and the Regulation of the Minister of Transportation Number 175 in 2015 [3] as recommended by PT. Industri Kereta Api (INKA) [4].

The loading conditions in the standard “UIC 566 1990-01-01 – Loadings of Coach Bodies and their Components” [2]. According to this standard, several forces occur on the train body components when running on the track, such as vertical, longitudinal, and transverse forces. The vertical force occurs due to gravity or the weight of the components on the car body itself, the longitudinal force occurs when starting and braking, while the transverse force is caused by the turning motion of the train when passing through a curve.

3 AC Frame Design and Modelling

The engineering drawing of the AC frame was designed and modeled using Autodesk Inventor software. The modeling process involved drawing the components of the AC frame, and the assembly process was carried out using a 3D model.

The AC frame has dimensions of 1900 mm length \times 1100 mm width \times 500 mm height, designed with a passenger capacity of 2 people and an operating speed of 40 km/h Fig. 1.

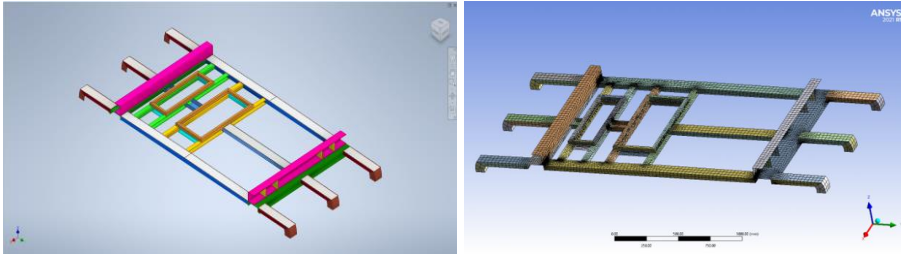


Fig. 1. (a) AC Frame Shunting Locomotive PPI (b) Meshing

3.1 Material

The required materials were based on the Regulation of the Minister of Transportation number 175 of 2015, where the base frame was designed with welded assembled steel construction made of carbon steel or other materials. That has high strength and stiffness against loading without permanent deformation and is equipped with impact-resistant construction. The material specified in the construction of this AC frame was Structural Steel SS400 (JIS G3101) for all main constructions in the form of plates and C profiles of the AC frame.

Table 1. Mechanical Properties [5]

| Elastic Modulus | Poisson Ratio | Density | Yield Strength | Ultimate Strength |
|-----------------------------|---------------|---------------------------|----------------|-------------------|
| 2,1 x 10 ⁵ (MPa) | 0,3 | 7850 (Kg/m ³) | 245 (MPa) | 400 (MPa) |

3.2 Meshing

The mesh used in this simulation had a size of 20 mm, producing 83,610 nodes and 28,288 elements. This site was considered comprehensive enough for modeling the AC frame. The mesh type used in this simulation was a hybrid mesh, consisting of quadrilateral and triangular shapes. The meshing used in the simulation was verified and validated using meshing testing parameters to ensure that the values generated by the software were close to the actual values. It provides accurate technical drawings and allows for visualization of objects in 3D Fig. 1b.

3.3 Determining Boundary Conditions and Load

The boundary condition will be determined by providing constraints. The constraint used in this simulation is a Fixed Support. This Fixed Support will be given a value of 0 on the X (longitudinal), Y (lateral), and Z (vertical) axes as well as rotation on the X (longitudinal), Y (lateral), and Z (vertical) axes.

This boundary condition will be applied to the legs of the AC frame that will be welded to the roof of the train, to limit the movement of the object being simulated. Fig. 2. (e), and table 5. explains the technical specifications AC frame.

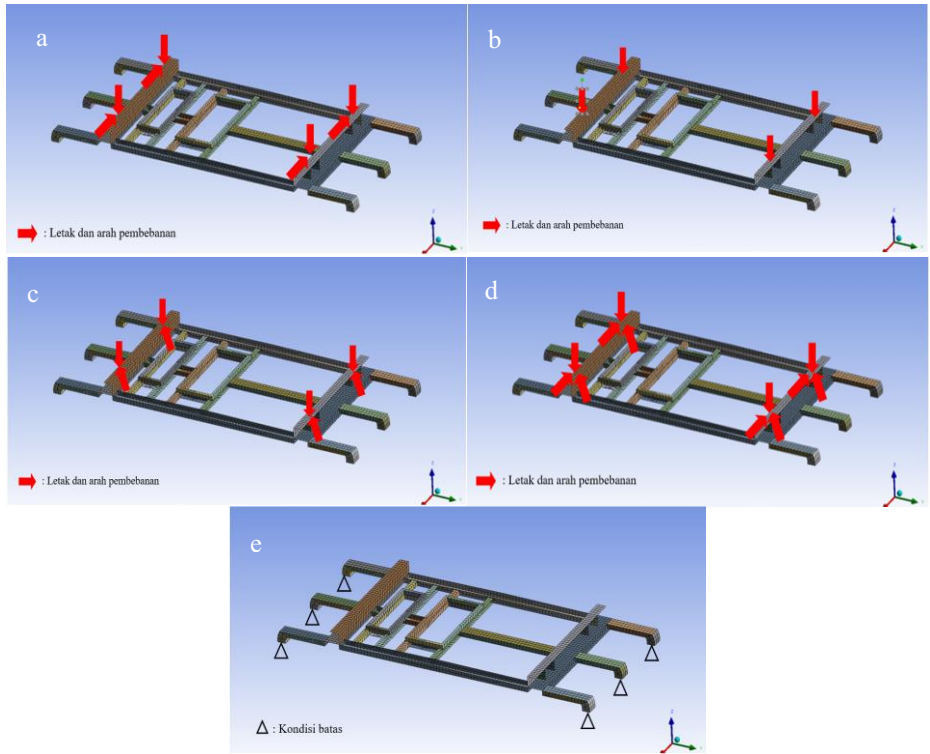


Fig. 2. (a) Vertical Load, (b) Vertical Transversal Load, (c) Vertical Longitudinal Load, (d) Combination Load, (e) Illustration of Boundary Condition.

Table 2. Technical Specifications AC Frame [2][4]

| Type | Specification | Mass (kg) |
|-----------|------------------------|-----------|
| Material | SS400 | |
| Dimension | 1900 x 1100 x 500 (mm) | 175 kg |

The load used in this simulation refers to the UIC 566 standard [2]. The main loading on the AC frame model was applied to the upper mounting frame of the AC as a vertical, lateral, and longitudinal load. The loads include:

1. Vertical load = $F_z = m.(g.a_z) = 175 \text{ kg} \times (9.8 \text{ m/s}^2 \times 2 \text{ m/s}^2) = 3,430 \text{ N}$
2. Longitudinal load = $F_x = m.(g.a_x) = 175 \text{ kg} \times (9.8 \text{ m/s}^2 \times 1.6 \text{ m/s}^2) = 2,744 \text{ N}$
3. Lateral load = $F_y = m.(g.a_y) = 175 \text{ kg} \times (9.8 \text{ m/s}^2 \times 1.5 \text{ m/s}^2) = 2,572.5 \text{ N}$

Each load is multiplied by the dynamic coefficient according to the UIC 566 standard. This ensures that the loads are applied during operational conditions. In Table 6., information is given regarding the forces that occur by the UIC 566 standard.

Table 3. Force on Bodies Component

| Force | Formulas | Calculation results |
|----------------------------|---|---------------------------------|
| Vertical | $a_z = 2 \text{ m/s}^2$ | |
| Transversally | $a_y = 1,5 \text{ m/s}^2$ | |
| Longitudinal | $a_x = 1,6 \text{ m/s}^2$ | |
| Vertical Load | $F_z = m.(g.a_z)$ | 3.430 N |
| Vertikal Transversal Load | $F_z = m.(g.a_z)$ $F_y = m.(g.a_y)$ | 3.430 N 2.572,5 N |
| Vertikal Longitudinal Load | $F_z = m.(g.a_z)$ $F_x = m.(g.a_x)$ | 3.430 N 2.744 N |
| Combination Load | $F_z = m.(g.a_z)$ $F_y = m.(g.a_y)$ $F_x = m.(g.a_x)$ | 3.430 N 2.572,5 N 2.744 N |

4 Research Results

The structural simulation results obtained include the stress distribution, maximum vertical deflection, and safety factor at each node. The von Mises stress was used to determine the stress distribution, as it is a failure theory that considers multiaxial stress.

The output values from this simulation will be used as a reference for analyzing the structural strength of the car body. According to the Minister of Transportation Number 175 of 2015, the maximum allowable stress is 75% of the Yield Strength Material used. For the SS400 material (JIS G3101) with a yield strength of 245 MPa, the maximum allowable stress is 183.75 MPa Fig. 3.

4.1 Von-Misses Stress

The following are the results of the Von-Misses Stress in Fig. 3.

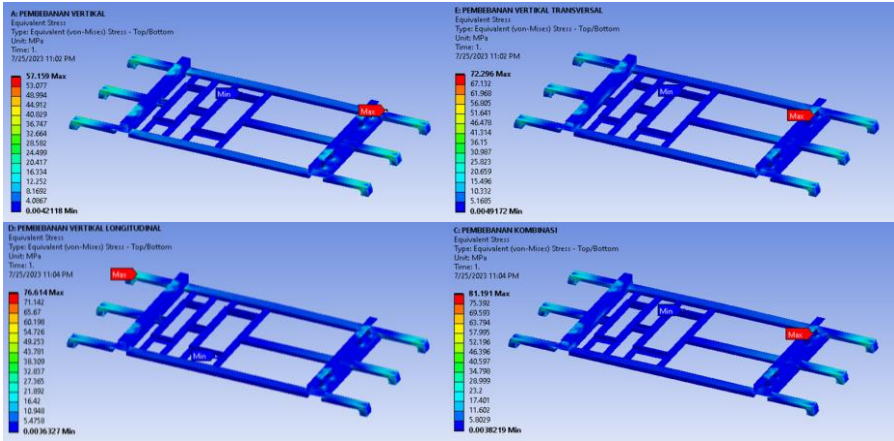


Fig. 3 Von Misses Stress (a) Vertical Load (b) Vertical Transversal Load, (c) Vertical Longitudinal Load, (d) Combination Load

From the simulation, it was found that the maximum stress that occurred due to the vertical load was 57.159 MPa on the sheeting bracket of the AC frame, due to the vertical longitudinal load was 72,296 MPa on the sheeting bracket of the AC frame. due to the case of vertical longitudinal loading 76,614 MPa on the sheeting bracket AC frame, was 81,191 MPa on the sheesheeting bracketframe.

4.2 Maximum Vertical Deflection

The following are the results of Maximum Vertical Deflection in Fig. 4.

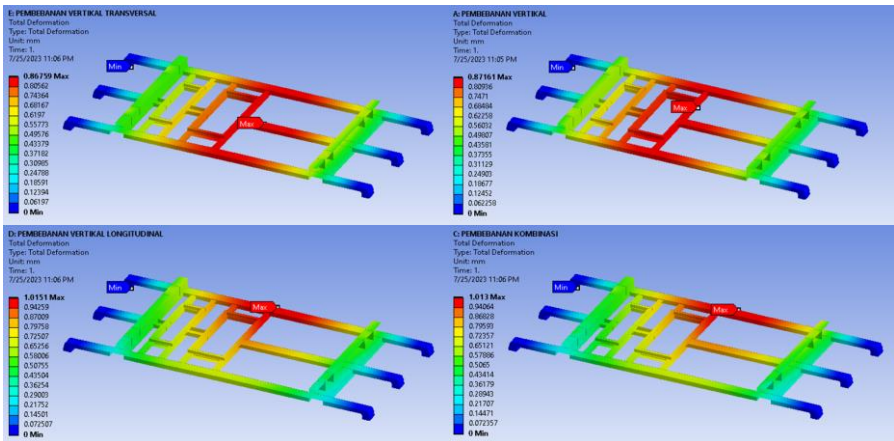


Fig. 4 Maximum Vertical Deflection (a) Vertical Load (b) Vertical Transversal Load, (c) Vertical Longitudinal Load, (d) Combination Load

From the simulation, it was observed that the maximum vertical deflection due to the vertical load occurring on the Y axis was 0.87161 mm on the purline frame, due to the vertical transversal load was occurred Y aatis was 0,86759 mm on the carline frame, due

to the vertical longitudinal load occurred was 1,051 mm on the carline frame, due to the combination load occurred on the carline frame.

4.3 Safety Factor

The following are the results of the vertical longitudinal loading simulation Fig. 5.

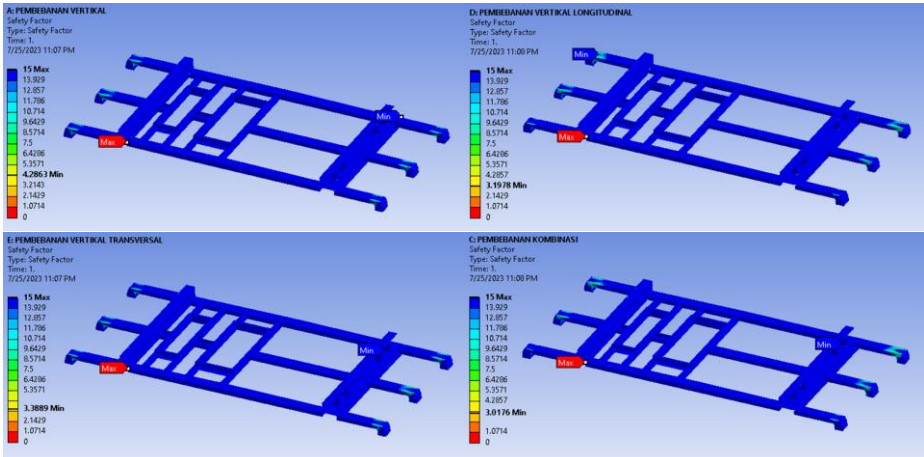


Fig. 5 Safety Factor (a) Vertical Load (b) Vertical Transversal Load, (c) Vertical Longitudinal Load, (d) Combination Load

From the simulation, it was found that the smallest safety factor value was 4.286 in the vertical load case, the smallest safety factor value was 3,389 on the vertical transversal load case, the smallest safety factor value was 3,197 on the vertical longitudinal load case, and the smallest safety factor value was 3,07 on the combination loading load case.

In Table 3, the difference in the error value between the two stress results that occur in each test can be seen. The largest error value occurred in the first loading variation, namely compression loading, with an error value of 1.99%. The data obtained from the simulation results are valid because the deviation and error values are still below <10% [7].

Table 4. Stress and Deflection Simulation Results

| No | Load Case | Deflection (mm) | Stress (MPa) | Location of Maximum Stress | Description |
|----|---------------|-----------------|--------------|----------------------------|--------------------------------------|
| 1 | Vertical Load | 0,87161 | 57,159 | Sheeting Bracket Frame AC | $\sigma_{max} < \sigma_{permission}$ |

| No | Load Case | Deflection (mm) | Stress (MPa) | Location of Maximum Stress | Description |
|----|----------------------------|-----------------|--------------|-----------------------------|--|
| 2 | Vertical Transversal Load | 0,86759 | 72,296 | Stiffener Frame Mounting AC | $\sigma_{\max} < \sigma_{\text{permission}}$ |
| 3 | Vertical Longitudinal Load | 1,0151 | 76,614 | Sheeting Bracket Frame AC | $\sigma_{\max} < \sigma_{\text{permission}}$ |
| 4 | Combination Load | 1,013 | 81,191 | Stiffener Frame Mounting AC | $\sigma_{\max} < \sigma_{\text{permission}}$ |

Table 5. Safety Factor Simulation Results

| No. | Load Case | Safety Factor | Location of Maximum Stress | Description |
|-----|----------------------------|---------------|-------------------------------|--------------------------------------|
| 1 | Vertical Load | 4,286 | <i>Sheeting Bracket Frame</i> | $sf_{\min} > sf_{\text{permission}}$ |
| 2 | Vertical Transversal Load | 3,389 | <i>Stiffener</i> | $sf_{\min} > sf_{\text{permission}}$ |
| 3 | Vertical Longitudinal Load | 3,197 | <i>Bracket Mounting</i> | $sf_{\min} > sf_{\text{permission}}$ |
| 4 | Combination Load | 3,017 | <i>Stiffener</i> | $sf_{\min} > sf_{\text{permission}}$ |

To validate the feasibility of meshing, this research uses a comparison between the results of manual/theoretical calculations which will later be compared with the results from the simulation. Apart from validation using a comparison of manual value results with simulated value results, a convergence test was also carried out to determine the best mesh size to use in testing. The convergence test is carried out by looking for a stable error value from the results of the first test to the results of the next test [6]. Then several parameters are also used in verifying whether the meshing used is suitable for use for simulation or not. The following is a table of validation and verification of meshing feasibility and also a comparison of theoretical calculation stress results with simulation results:

Table 6. Verification of Ansys Meshing Simulation

| No. | Parameter | Results | Value | Description |
|-----|----------------|---------|----------|-------------|
| 1 | Skewness | 0,169 | 0 – 0,25 | Excellent |
| 2 | Jacobian Ratio | 1,319 | 1 - 10 | Excellent |

Table 7 Validation of Ansys Meshing Simulation

| No | Parameter | Theoretical calculation results | Ansys simulation results | Difference | Information Error |
|----|------------------------|---------------------------------|--------------------------|------------|-------------------|
| 1 | Numerical Calculations | 16,978 Mpa | 17,324 Mpa | 0,346 | 1,99 % |

Table 8 Mesh Convergence

| No. | Parameter | Mesh | Stress (Mpa) | Difference | Information Error |
|-----|------------|-----------------|--------------|------------|-------------------|
| 1 | Convergent | Between 20 - 80 | 56,3 – 57,3 | 1 | 0,73% |

5 Conclusions

From the simulation, it was found that the maximum von Mises stress that occurred under the combined loading condition on the stiffener frame of the AC was 81.2 MPa. This stress value represents 33.14% of the yield strength of the SS400 material, which is 245 MPa. The results were considered safe as the percentage was below the 75% limit specified in the Minister of Transportation Regulation Number 175 of 2015. Additionally, the simulation revealed a maximum vertical deflection of 1.015 mm due to the resultant forces from the longitudinal vertical load of the air conditioning system. The minimum safety factor obtained from the simulation was 3.01, which is still categorized as safe according to the UIC 566 standard, which sets a minimum safety factor of 1.6 for welded frame structures. Overall, the simulation results indicate that under all loading conditions, the structure remains within safe limits according to the applicable standard.

References

- [1] Menteri Perhubungan RI, “Peraturan Menteri Perhubungan Republik Indonesia Nomor Pm 16 Tahun 2022 Tentang Rancang Bangun Dan Rekayasa Sarana Perkeretaapian,” no. 856. Kementerian Perhubungan Republik Indonesia, 2022.
- [2] U. I. des C. de Fer, “UIC 566 Loading of Coach Bodies and Their Components,” *International Union of Railways*. International Union of Railways, 1990.
- [3] Menteri Perhubungan RI, “Standar Spesifikasi Teknis Kereta Kecepatan Normal Dengan Penggerak Sendiri,” vol. 2015. Kementerian Perhubungan Republik Indonesia, pp. 1–32, 2015.
- [4] P. INKA, “Spesifikasi Teknis Peralatan Sarana Penggerak TMC.pdf.” 2022.
- [5] S. Team, “Baja SS400,” *steelindopersada.com*, 2015.

- <https://www.steelindopersada.com/2015/03/ss400-structural-steel-bukan-stainless-steel.html>
- [6] W. Artha Wirawan, F. Pandu Wijaya, D. Sanjaya Atmaja, F. Rozaq, A. Satria Bagaskara, and F. X. Prakosa Pamungkas, *Modelling and Structural Analysis of Tram Railway Vehicle Body with Finite Element Method*, vol. 1. Atlantis Press International BV, 2022. doi: 10.2991/978-94-6463-126-5.
- [7] W. Puji, D. Wulandani, and Y. A. Purwanto, “Kajian Pola Sebaran Aliran Udara Panas pada Model Pengering Efek Rumah Kaca Hibrid Tipe Rak Berputar Menggunakan Computational Fluid Dynamics,” *J. Enj. Pertan.*, vol. 7, no. 2, pp. 105–113, 2009.
- [8] W. Artha Wirawan, A. Zulkarnain, H. Boedi Wahjono, Jamaludin, and A. Tyas Damayanti, “The Effect of Material Exposure Variations on Energy Absorption Capability and Pattern of Deformation Material of Crash Box of Three Segments,” *J. Phys. Conf. Ser.*, vol. 1273, no. 1, 2019, doi: 10.1088/1742-6596/1273/1/012081.
- [9] S. Widi Astuti, W. Artha Wirawan, A. Zulkarnain, and D. Tri Istiantara, “Comparison of Energy Absorption and Pattern of Deformation Material Crash Box of Three Segments with Bilinear and Johnson Cook Approach,” *J. Phys. Conf. Ser.*, vol. 1273, no. 1, 2019, doi: 10.1088/1742-6596/1273/1/012078.
- [10] L. M. Khakim, “Analisis Dan Optimasi Desain Underframe Kereta Langsir Di Pt Inka (Persero),” 2022.

Open Access This chapter is licensed under the terms of the Creative Commons Attribution-NonCommercial 4.0 International License (<http://creativecommons.org/licenses/by-nc/4.0/>), which permits any noncommercial use, sharing, adaptation, distribution and reproduction in any medium or format, as long as you give appropriate credit to the original author(s) and the source, provide a link to the Creative Commons license and indicate if changes were made.

The images or other third party material in this chapter are included in the chapter's Creative Commons license, unless indicated otherwise in a credit line to the material. If material is not included in the chapter's Creative Commons license and your intended use is not permitted by statutory regulation or exceeds the permitted use, you will need to obtain permission directly from the copyright holder.

